UCRL-TR-210223

LAWRENCE
LIVERMORE
NATIONAL
LABORATORY

Diode-Pumped Alkali Atom Lasers

03-LW-024 Final Report

Ralph H. Page, Raymond J. Beach

February 16, 2005

Disclaimer

This document was prepared as an account of work sponsored by an agency of the United States Government. Neither the United States Government nor the University of California nor any of their employees, makes any warranty, express or implied, or assumes any legal liability or responsibility for the accuracy, completeness, or usefulness of any information, apparatus, product, or process disclosed, or represents that its use would not infringe privately owned rights. Reference herein to any specific commercial product, process, or service by trade name, trademark, manufacturer, or otherwise, does not necessarily constitute or imply its endorsement, recommendation, or favoring by the United States Government or the University of California. The views and opinions of authors expressed herein do not necessarily state or reflect those of the United States Government or the University of California, and shall not be used for advertising or product endorsement purposes.

This work was performed under the auspices of the U.S. Department of Energy by University of California, Lawrence Livermore National Laboratory under Contract W-7405-Eng-48. The project 03-LW-024 was funded by the Laboratory Directed Research and Development Program at LLNL.

Diode-Pumped Alkali Atom Lasers
03-LW-024 Final Report

Ralph H. Page and Raymond J. Beach
14 Feb 05

I. Introduction

The recent work at LLNL on alkali-atom lasers has been remarkably successful and productive. Three main phases (so far) can be identified. First, the concept and demonstration of red lasers using (Ti:sapphire pumping) took place; during this time, Rubidium and Cesium resonance-line lasers were tested, and theoretical models were developed and shown to describe experimental results very reliably. Work done during this first phase has been well documented, and the models from that period are still in use for their predictions and for designing power-scaled lasers. [1 - 3] Second, attempts were made to produce a blue alkali-vapor laser using sequentially-resonant two-step pumping (again, using Ti:sapphire lasers.) Although a blue laser did not result, the physical limitations of our approach are now better-defined. Third, diode-pumped operation of a red laser (Rubidium) was attempted, and we eventually succeeded in demonstrating the world's first diode-pumped gas laser. [4] Because we have a defensible concept for producing an efficient, compact, lightweight, power-scaled laser (tens of kW,) we are in a position to secure outside funding, and would like to find a sponsor. For descriptions of work done during the "first phase," see References [1 – 3.] "Phase two" work is briefly described in the section "Blue laser," and "phase three" work is presented in the section entitled "Diode-pumped red laser."

II. Blue laser

The red alkali-vapor lasers appear to behave rather predictably—their spectroscopy and kinetics are understood in great detail, and only three energy levels appear to matter. [1 – 3] A higher level of risk was involved in proposing a blue laser, since there are additional levels, additional relaxations, many more fluorescence and energy-flow pathways, and the average level of excitation (i.e. "temperature") of a lasing vapor would have to be much higher. Figure 1 sketches the dominant population flows that would hypothetically occur ina working blue alkali-vapor laser.

Unexpected fluorescence transitions observed

We conducted experiments designed to produce laser emission on the blue Rb lines near 421 nm. Watt-level Ti:sapphire lasers were tuned to sequentially populate the first- and second-excited P levels. (There are various wavelength combinations that accomplish this; they all work.) A fluorescence spectrum (Figure 1(b)) indeed shows blue emission, showing that the pump lasers were tuned correctly. There are other signals as well—note the 7s – 5p transitions near 730 – 740 nm. Also, there is a broad band (tentatively assigned to dimer emission) near 550 nm. In fact, viewing the glow (Figure 2) through a yellow filter (that cuts blue) enables one to see the yellow color quite clearly.

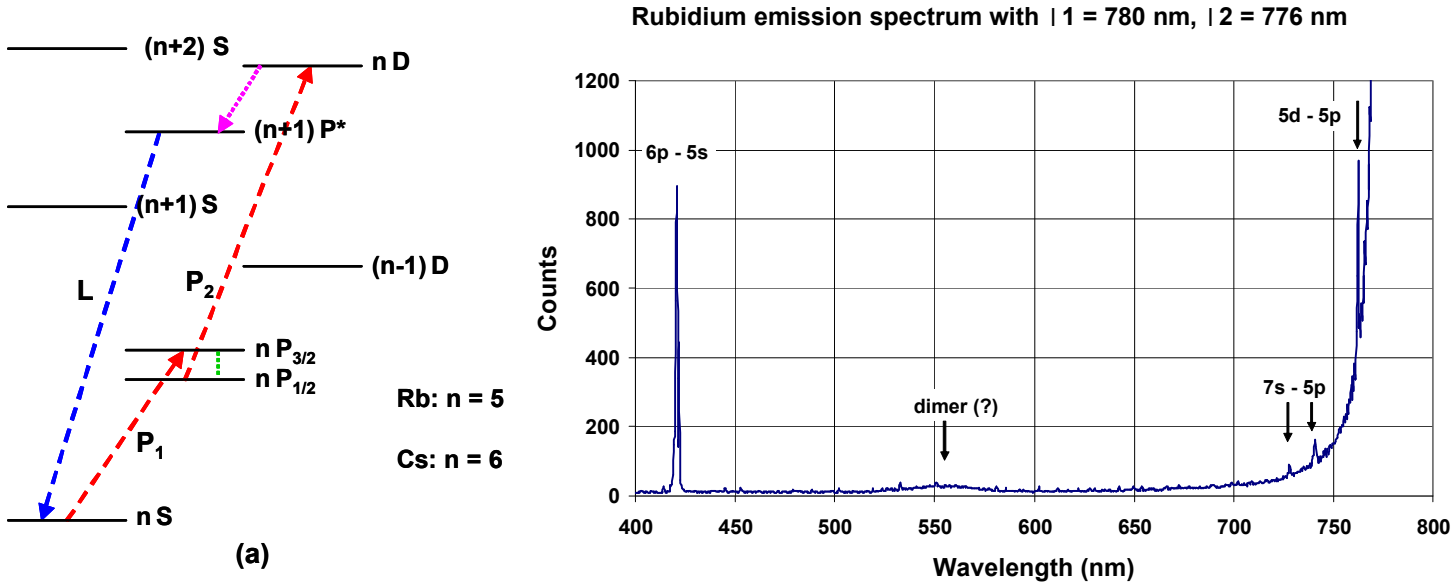

Figure 1. (a) Energy levels and transitions in a working blue alkali-vapor laser. P_1 and P_2 are respectively the first- and second-step pump transitions, and L is the laser transition. Thermal relaxation within the first-excited-state manifold is shown in green, and collisionally-induced relaxation to populate the upper laser level is shown in magenta. In practice, all levels shown in this diagram are populated to some extent. (b) fluorescence spectrum observed with Rb vapor in He (with ethane added to facilitate relaxation.)

Visibility of emissions from the 5d and 7s levels is a clue that relaxation into the 7p level is not as effective as we would like. Some workers have found that addition of electronegative buffer gases (like CO and N2) facilitates inter-level relaxation, and we configured our gas manifold to deliver these additional gases to the cell.

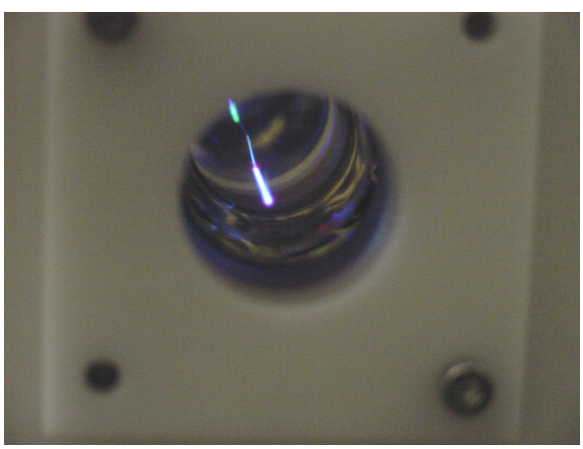

Figure 2. Glow seen in 1-inch Pyrex Rb cell undergoing 2-color pumping to populate upper level for blue-laser operation.

IR branches have much-larger cross sections than the desired blue line

While seeking to understand the failure of the "blue Rb laser" to lase, another fact came to light—the IR fluorescent branches (not shown) from (n+1)P to (n+1)S and (n-1)D are much more powerful than the one we attempted to use for the laser transition. Whereas the "red laser" transitions have near-unit oscillator strength, the "second resonance" (blue) line is weaker by roughly 2 orders of magnitude. The longer-wavelength transitions are preferred, and their cross section scales as the square (or even a higher power) of the wavelength, giving them a greatly-reduced oscillation threshold. (Since those transitions don't terminate on the ground level, bottlenecking could be a problem.)

Laser attempt with Cesium

Our frustration over the situation with Rubidium led us to turn to Cesium. Because the spacings between various energy levels are different in the two atoms, some of the kinetic processes have different rates and different probabilities, perhaps making it more likely that Cs would work. So, we swapped vapor cells, cavity optics, and pump-laser wavelengths. Still, in spite of making blue (455 nm) fluorescence, we were not able to establish blue-laser operation with a "standard" vapor cell (that includes metal, ~100 torr ethane, and ~0.66 atm He.)

Significant second-step pressure broadening

One variable that is important in governing the operation of the blue-laser schemes is the strength of the "second-step" pump transition (P_2 in Fig. 1.) Its oscillator strength is known, but its peak cross section depends on its linewidth, which is governed by pressure broadening. Because this transition occurs between two excited states, it is not observed in ordinary absorption spectra. To our knowledge, the pressure-broadening rate for this transition has not been reported (although many higher Rydberg states have been studied using laser spectroscopy.) We decided to check it using the LIF (Laser-Induced Fluorescence) technique, of recording the blue fluorescence strength *vs* the second pump frequency. The observed spectrum is Figure 3, and the Lorentzian fit has a FWHM linewidth parameter of 2.5 cm^{-1}.

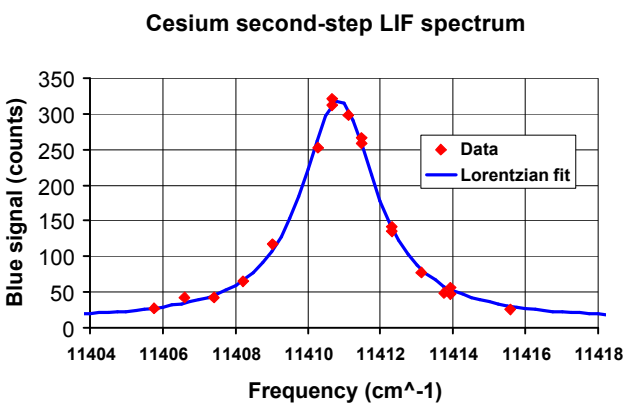

Figure 3. Laser-induced fluorescence spectrum of the Cs 6p – 6d transition used to excited Cs atoms above the blue-emitting 7p level. The inferred linewidth (for a ~ 1 atm He + ethane mixture) is ~ 75 GHz.

This linewidth is a few times larger than that of the first-step transition (whose broadening rate is ~ 18 GHz/atm.) Coupled with its smaller oscillator strength (roughly a factor of 2,) this transition has nearly one-order-of-magnitude lower peak cross section.

Assessment of the spectroscopy and kinetics

Based on our integrated knowledge of the oscillator strengths, linewidths, etc. we conclude that in the pressure-broadened regime, the peak cross sections for the P_1, P_2, and L transitions are roughly in the ratio 100 : 10 : 1. In this same scheme, the "parasitic" transitions (n+1)P – (n+1)S, (n-1)D have peak cross sections in the range ~ 10 – 100, making it likely that they would reach "threshold" well before the blue transition would lase. So, the prospects for a diode-pumped blue alkali laser are not as promising

as those for the red laser. This is not to say it is impossible, just rather challenging. Creation of an efficient blue alkali laser would probably involve

- Hard pumping on the first-step pump transition (to deplete the ground state,)
- Very-hard pumping on the second-step pump transition (since its cross section is low,)
- Very-low intracavity loss (and low output coupling, at most a few percent) at the blue-laser wavelength (because the emission cross section is low and the attainable gain is small,)
- Quenching of the IR "parasitic" transitions,
- Optimization of nD – (n+1)P population transfer by selection of buffer gas.

Superfluorescent blue emission from Cesium

Since we had a tubulated glass cell at our disposal, and a gas-handling manifold with which to charge it, we were able to explore various combinations of buffer gas, fill pressure, etc. While pumping with the two Ti:sapphire lasers, we introduced (and evacuated) such gases as He, N_2, and CO. Eventually, we created a bright blue spot (Figure 4) on a card roughly one foot from the vapor-cell housing. The spot was small, typical of coherent emission with a Rayleigh range similar to that of the pump lasers.

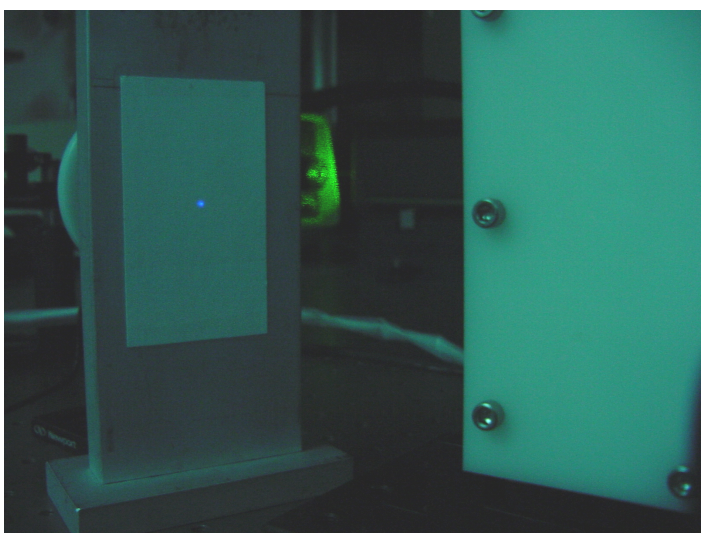

Figure 4. Bright blue (455 nm) collimated emission, roughly 1 μW, obtained while pumping Cs vapor with two Ti:sapphire lasers. The cell was at a low pressure, very probably in the Doppler-limited regime.

The blue spot appeared when the cell was near vacuum. In this circumstance, we suppose that pressure-broadening of the transitions was not occurring, so that peak cross sections for the various transitions would be maximized, and more-nearly-equal in value. Also, with narrow linewidths, "optical path density" (number of nepers of absorption or gain) would also be quite large. By pumping with high-beam-quality, powerful, narrowband Ti:sapphire lasers, the pump intensities in the vapor cell would many-times-over exceed the alkali-vapor saturation intensities. So, we believe that we achieved at least superfluorescent emission, and perhaps even lasing (albeit at the microwatt level.) Therefore, it is concievable that a blue alkali laser will someday be built. However, the conditions required for this accomplishment were quite specialized and unfortunately, we haven't reproduced the result.

III. Diode-pumped red laser

The resounding success of the campaign to demonstrate alkali-vapor lasers (using Ti:sapphire pump lasers) led to high confidence in our ability to design diode-pumped alkali-vapor lasers. Diode-pumping is highly preferred for its economy, simplicity, efficiency, and compactness, and would presumably be required in a practical system. By "diode-pumping" we mean use of high-power arrays (not single-spatial-mode low-power diodes, whose beams are not all that different from those of Ti:sapphire lasers.) In general, the pump light from arrays is broadband, multiple-spatial-mode, and nowhere near as bright as a Ti:sapphire laser. Much of the challenge in getting a DPAL (Diode-Pumped Alkali Laser) to work is in producing a high pump spectral density (well above the saturation intensity) over the length of the vapor.

Diode-array properties

Getting the first DPAL to work was very slow going, during which time we put much effort into characterizing the pump-diode arrays. The Coherent "FAP" arrays produce their output via a bundle of 19 fibers, each ~140 μm in diameter, for a total bundle diameter of ~800 μm, as shown in Figure 5 (a).

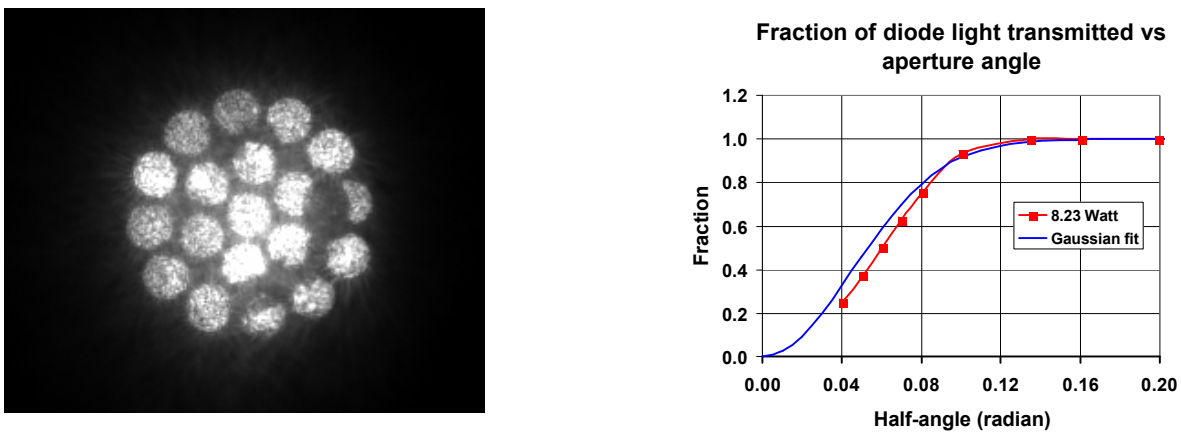

(a) (b)

Figure 5. (a) Image of output end of Coherent "FAP" array, showing 19 fibers arranged in a 1 – 6 – 12 pattern. Overall width of the bundle is ~800 μm. (b) Measurement of the fraction of diode-array light collected *vs* angle. A Gaussian fit (obviously imperfect) of angle-parameter 0.9 radian is superposed. The NA appears to be close to 0.12.

An important parameter is the numerical aperture (NA) of the source; according to the manufacturer's data, this is 0.12, roughly in agreement with the data of Figure 5(b.) For purposes of calculations and comparison with single-mode laser beams, it is helpful to have a Gaussian fit parameter, and in this case, that number is 0.09 radian. Given the spot size and divergence, this array's output is a few hundred times diffraction limited (in each axis.)

Because DPAL operation involves saturating (bleaching) at atomic transition (whose linewidth is small,) we are interested getting a high pump power at the pump transition's wavelength (780.25 nm, in the case of Rubidium.)

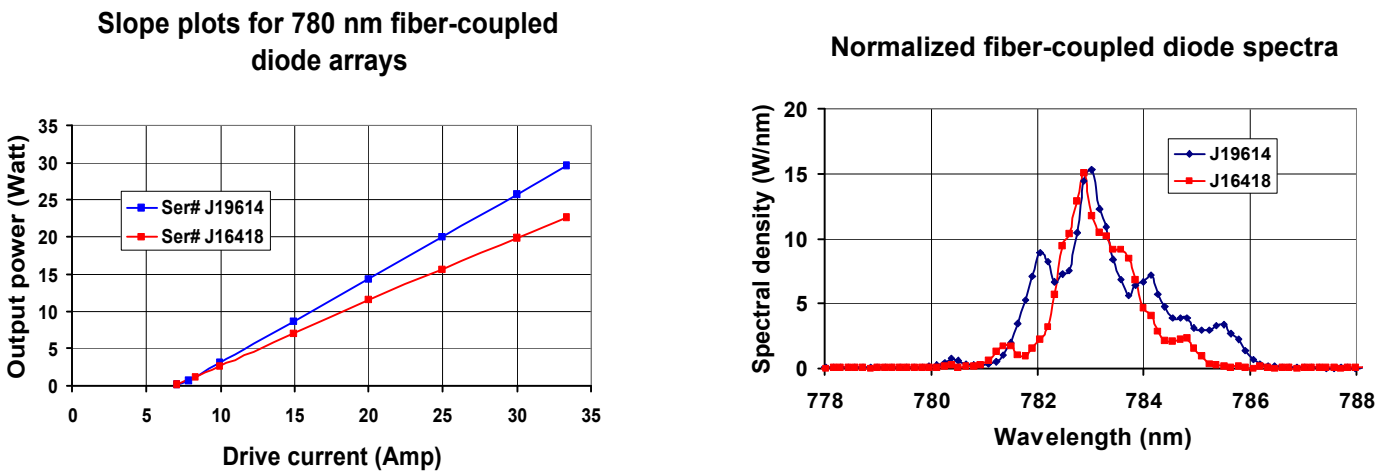

Figure 6. (a) Slope plots for each of two FAP arrays we used for pumping a Rb DPAL. (b) Normalized power spectra for each of the arrays. The array with more power also had a larger effective linewidth, such that each had a similar peak power density.

Our data showing the total power and spectrum for each of the two FAP arrays on hand is shown in Figure 6. Note that the diodes are set at the desired wavelength by temperature-tuning via the water-cooling lines. The key result of all this characterization is that each array could produce 15 W/nm in a 0.8 mm spot with a numerical aperture of 0.12. The "confocal distance" in this case is only a few mm, and because the brightness was not as high as desired, telescoping of the diode output was required to reduce the spot size (and further shortne the confocal distance.)

Other testing we performed on the diodes showed that their polarization purity was not so high—roughly 2:1. So, polarization-combining was inherently wasteful.

First DPAL setup

Our modeling results suggested that the Rb laser threshold could be reached (barely) with the pump power available with the diode arrays, if their outputs were combined. The cavity was designed around a heated vapor cell based on uncoated-sapphire-window Conflat viewports (Figure 7.) Because the pump confocal distance was short, we sought a short vapor path length. Using available hardware, 6 mm was the smallest gap that was easily produced. The cell was placed at the center of a nearly-confocal cavity with 20 cm radius mirrors. The closeness of the pump and laser wavelengths made end-pumping unrealistic, since the mirrors would attenuate the pump light; therefore, side-pumping was used. To avoid polarization-rotation effects, we used a "holey mirror" (protected silver) with a 1.5 mm hole to reflect most of the pump light sideways, and transmit the resonated laser beam. The diode-array beams were polarization-combined (with significant loss) and down-telescoped in diameter a factor of 0.75. Overall, the pump delivery efficiency from diode array to inside the cell was only ~0.54.

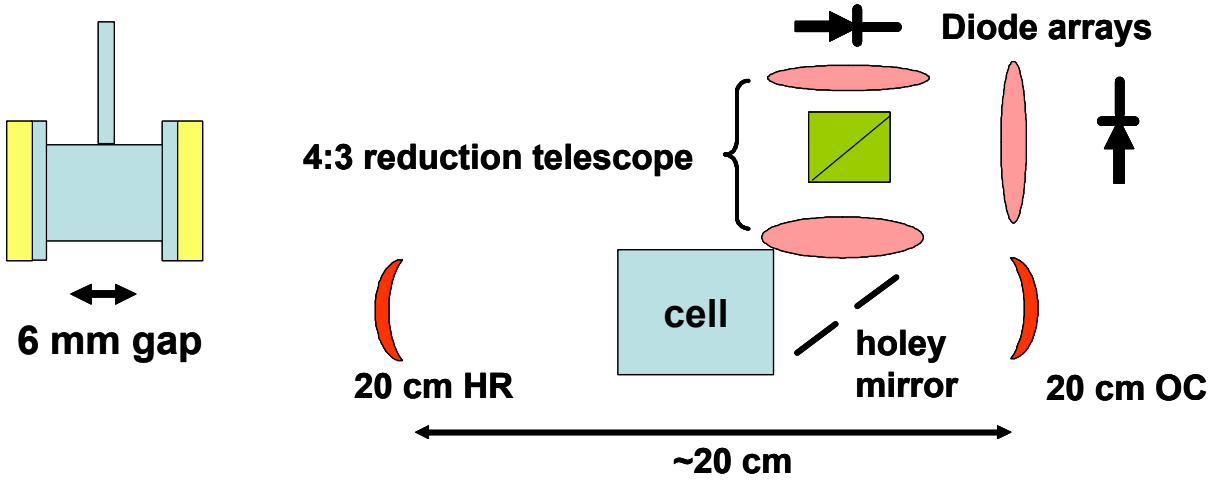

Figure 7. First diode-pumped alkali-laser setup using a "holey mirror" to transport the polarization-combined, down-telescoped outputs of two diode arrays into the center of a vapor cell with 6 mm gap.

Systematics

A key variable in the alkali-vapor-laser system is the pump absorption per pass (in "nepers,") commonly written as **N**s**L**, where **N** is the vapor number density, **L** is the cell gap length, and s is the absorption cross section. The cross section is pressure-dependent, and the number density is temperature-dependent. To avoid attempting laser operation with a gross departure from "optimum" (least threshold, around 10 neper pump absorption,) we did a check on the resonance-line absorption (both D_1 and D_2 lines) using a Rb hollow-cathode discharge lamp. Upon doing so, we found that we obtained consistent results from both lines, and that the absorption was higher than expected (perhaps because of under-filling with helium.) We reduced the cell temperature accordingly, and used various values starting with 130 C. A spectrum of the transmitted pump light is shown in Figure 8. The dip (very under-resolved) slightly above 780 nm is evidence of the pump absorption. Note that most of the pump light is wasted, since the pump spectrum is very broad compared with the atomic linewidth. Also, there is a small but important fluorescence signal at 795 nm—this is the Rb D_1 line, which is the laser transition. The 780 nm notch and 795 nm peak are signatures of the presence of Rb vapor, not to be taken for granted, since the metal reacts quickly with oxygen, water, etc. and will be completely consumed if the cell leaks.

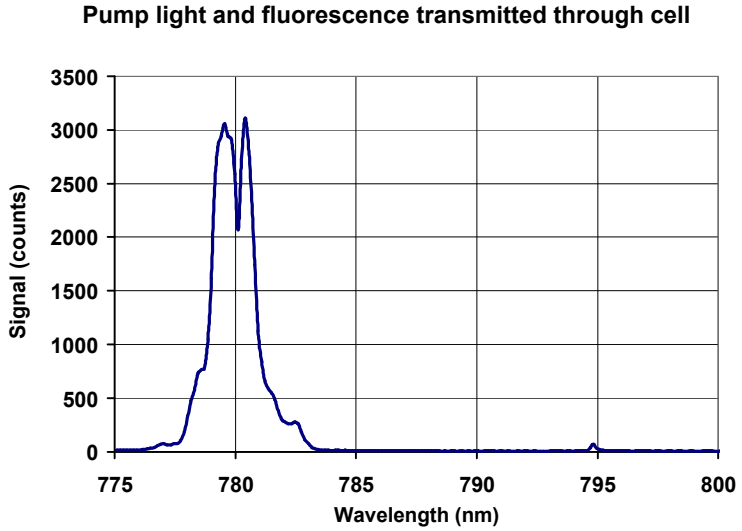

Figure 8. Spectrum of transmitted pump light (see notch near 780 nm) and Rb fluorescence (small peak at 795 nm.)

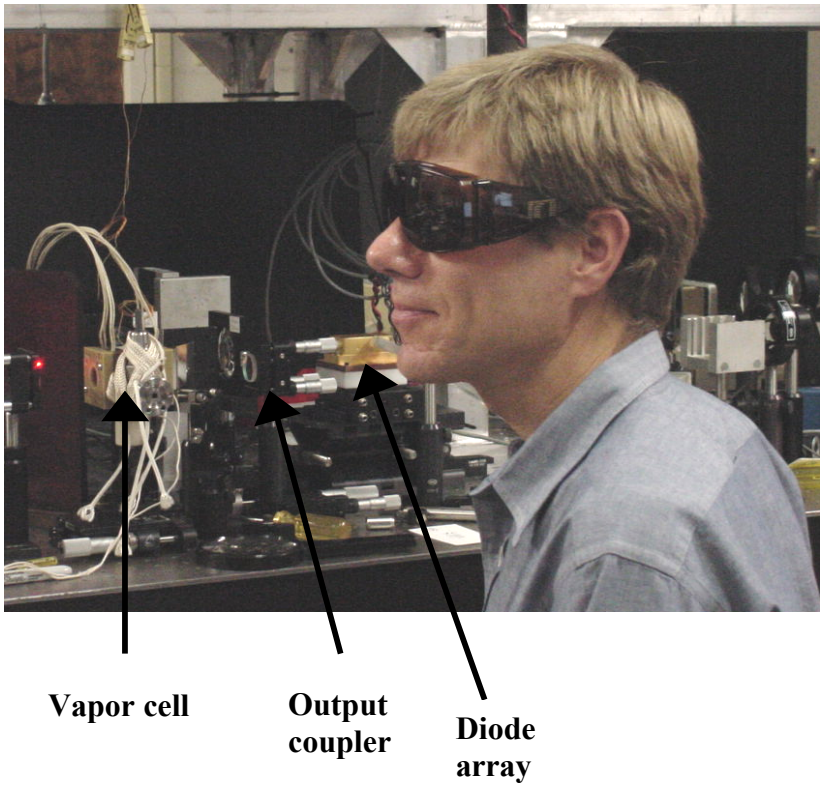

Figure 9. DPAL laboratory, laser setup, and laser experimenter. The vapor cell is covered in heater tape, and its assembly is mounted on translation stages to facilitate alignment to the pump-diode beam. One of the diode arrays is visible; the other is hidden behind other components of the setup.

DPAL operation demonstrated

Figure 9 is a photograph of the laboratory taken on 16 Nov 04, the day the diode-pumped laser first worked, showing the vapor cell, output coupler, one diode array, and an experimenter. In the first experiments, cell temperatures near 130 C were used. The laser output was detected through a 795 nm interference filter that rejected a strong background of 780 nm pump light. Output powers ranging up to 1 mW were observed, but in general, lasing was erratic. It was possible to sustain laser operation over a wide temperature range, as expected. Viewed with an IR camera, the output spot was round and filled-in—apparently, the classic fundamental Gaussian mode, as expected.

Evolving toward more-efficient operation

The marginal performance of the first DPAL was not a surprise, because the struggle to reach laser threshold had taken so long, and because our design models and experience pointed out several hindrances. The need for high pump intensity all the way through the vapor path was recognized, and we knew it would be helpful to shorten the cell to 2 or 3 mm to maintain high intensity at the ends of the path. Also, the cell windows, being uncoated sapphire, introduced significant loss—roughly 6% per surface (for each of 4 surfaces.)

A new cell was designed in which the sapphire viewports were oriented "backwards," so that the gap between the windows was only about 2 mm. Prior to assembly, the windows were anti-reflection coated on all surfaces. The new cell was compatible with the old holder, which furnished temperature control. Significant degradation of the cell transmittance occurred during use, but while it was new, laser operation was considerably easier to obtain and much more steady than with the old cell. A slope plot taken at 140 C cell temperature is shown in Figure 10. This plot does not

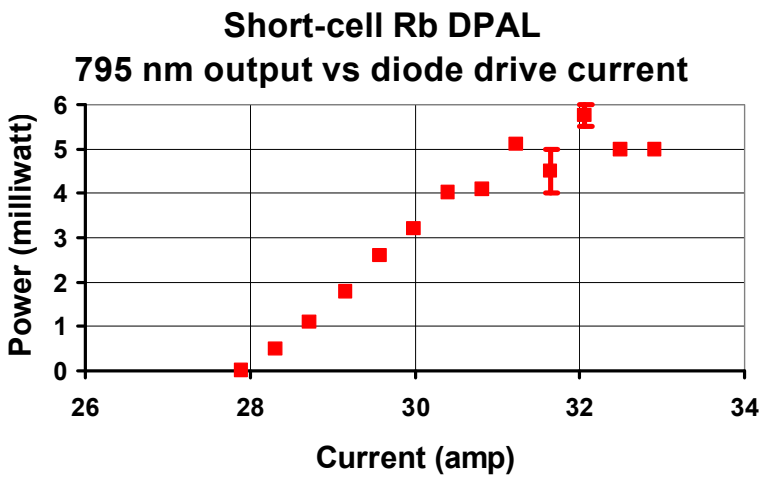

Figure 10. Slope plot for new laser cell with 2 mm gap and AR-coated windows. The actual threshold could be lower than shown if the diode temperature were adjusted at each current setting.

tell the whole story, because changing the diode drive current also changes the array heating, and thus the output wavelength. (The array spectrum is only "spot-on" at the highest current.) Thus, the threshold is much lower than one would be led to believe from this plot. In fact, when running at maximum current, laser operation was achieved with either pump-array independently (by blocking the other one.) Observed output powers ranged up to ~7 mW (uncorrected for filter transmision) and in reality, exceeded 10 mW. As with the longer cell, laser operation could be achieved for a wide range of cell temperatures.

Performance projections

Considering the large amount of diode-array pump power available, laser powers in the mW range appear disappointing at first blush. However, only a small fraction of the pump light is absorbed in the metal vapor, so much of the perceived shortfall can be rationalized. The AR coating on the sapphire windows (presumably MgF_2) appears to degrade in the region where the pump light passes, raising the intracavity loss and reducing the pump transmittance significantly. To help demonstrate better performance, we exercised the laser model for a series of temperatures, and the available values of output coupling. (Data above were obtained under non-optimum conditions—94% reflectivity, cell temperature 140 C.) The plots in Figure 11 show how the expected laser

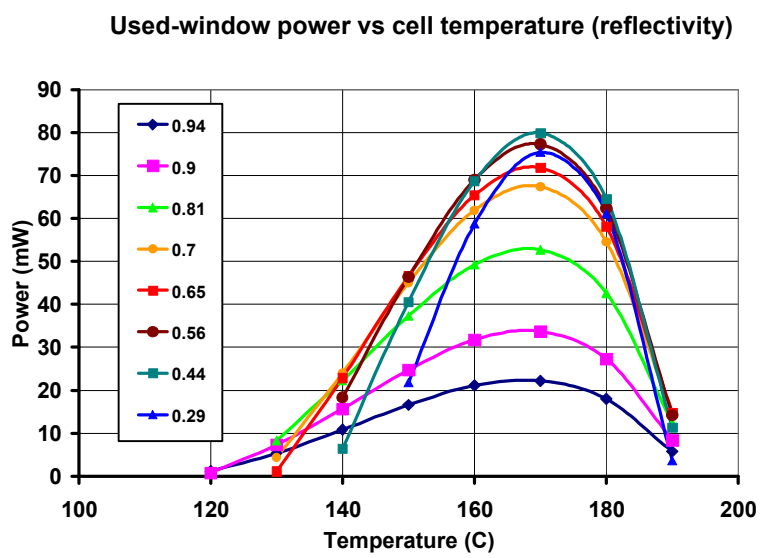

Figure 11. Projected laser output with one diode array and degraded window coatings, for a series of cavity reflectivities and cell temperatures.

output varies with these parameters, in the case that the cell window's coatings have degraded. It is assumed that the cell is charged with 1 atm He (similar to what has been in use) and that only one diode array is used for pumping. The broad maximum near 170 C (for nearly all values of output coupling) reflects the facts that (1) intracavity loss is a significant fraction of the total loss including useful output, and (2) there is a tradeoff between increased pump absorption, and higher threshold (more vapor to bleach) as the temperature is raised. Each 10 C increment in temperature changes the Rb number density by roughly a factor of 2.

Power scalability

The future for DPALs is promising. Reference [3] includes a discussion of a 100 kW system produced with a diode-pumped unstable resonator whose gas fill need not flow in order to manage the heat produced in the vapor. We can expect to see many exciting developments of this technology in the years to come.

References

[1] William F. Krupke, Raymond J. Beach, V. Keith Kanz, and Stephen A. Payne, "Resonance transition 795-nm rubidium laser," Optics Lett. **28**, 2336 (2003.)

[2] R. J. Beach, W. F. Krupke, V. K. Kanz, and S. A. Payne, "End-pumped 895 nm Cs laser," UCRL-CONF-155865; Advanced Solid-State Photonics 2004, Santa Fe, New Mexico, February 1 – 4, 2004.

[3] Raymond J. Beach, William F. Krupke, V. Keith Kanz, Stephen A. Payne, Mark A. Dubinskii, and Larry D. Merkle, "End-pumped continuous-wave alkali vapor lasers: experiment, model, and power scaling," J. Opt. Soc. Am. B **21**, 2151 (2004.)

[4] Ralph H. Page, Raymond J. Beach, V. Keith Kanz, and William F. Krupke, "First demonstration of a diode-pumped gas (alkali vapor) laser," UCRL-CONF-208239; submitted to CLEO/QELS 2005, Baltimore, Maryland, 22 – 27 May, 2005.